

Lepton flavor violating dark photon

Alexey S. Zhevlakov ^{*,1,2} Dmitry V. Kirpichnikov ^{†,3} and Valery E. Lyubovitskij ^{‡4,5,6}

¹*Bogoliubov Laboratory of Theoretical Physics, JINR, 141980 Dubna, Russia*

²*Matrosov Institute for System Dynamics and Control Theory SB RAS,
Lermontov str., 134, 664033, Irkutsk, Russia*

³*Institute for Nuclear Research of the Russian Academy of Sciences, 117312 Moscow, Russia*

⁴*Institut für Theoretische Physik, Universität Tübingen,
Kepler Center for Astro and Particle Physics,
Auf der Morgenstelle 14, D-72076 Tübingen, Germany*

⁵*Departamento de Física y Centro Científico Tecnológico de Valparaíso-CCTVal,
Universidad Técnica Federico Santa María, Casilla 110-V, Valparaíso, Chile*

⁶*Millennium Institute for Subatomic Physics at the High-Energy Frontier (SAPHIR) of ANID,
Fernández Concha 700, Santiago, Chile*

(Dated: December 20, 2023)

We study the possible impact of dark photons on lepton flavor phenomenology. We derive the constraints on non-diagonal dark photon couplings with leptons by analyzing corresponding contributions to lepton anomalous magnetic moments, rare lepton decays and the prospects of fixed-target experiments aiming for search for light dark matter based on missing energy/momentum techniques.

I. INTRODUCTION

Direct search for dark matter (DM) remains one of the most challenging issues in particle physics. Astrophysical data and cosmological observations at different scales imply the indirect evidence of DM. Despite numerous intensive direct searches for DM in the accelerator based experiments, little is known about origin and dynamics of weakly coupled particles of the hidden sector. In addition, the muon ($g-2$) anomaly [1] and recent tensions between Standard Model (SM) expectation and experimental measurements [2–5] have been stimulated a development of various beyond SM (BSM) scenarios involving sub-GeV hidden sector particles [6].

Typically such scenarios imply a feebly interacting mediator (portal) states connecting the BSM sector with SM particles. In particular, recently several such hidden sector scenarios have been discussed in literature: the Higgs portal [7–9], the tensor portal [10–12], the dark photon portal [13–15], sterile neutrino portal [16], axion portal [17], and Stueckelberg portal [15, 18].

It is worth noticing that some hidden sector models suggest an idea of lepton non-universality and lepton flavor violation (LFV). In this sense, a light sub-GeV hidden particles may potentially explain a muon ($g-2$) anomaly and other SM tensions in particle physics implying LFV effects [19–23]. We note that neutrino oscillations provide clear experimental evidence for LFV, however for the charged lepton sector these effects are strongly suppressed. Therefore, in order to probe LFV phenomena one may address a new light vector field that violates charged lepton flavor at tree level. To be more specific,

in the present paper, we discuss the examination of dark photon portal that can be relevant for LFV lepton decays and LFV processes at fixed target experiments.

In case of dark photon, which can acquire a mass via the Stueckelberg mechanism, the Lagrangian of its interaction with DM can be written as follows [15]

$$\begin{aligned} \mathcal{L}'_{\text{DS}} = & -\frac{1}{4} A'_{\mu\nu} A'^{\mu\nu} + \frac{m_{A'}^2}{2} A'_\mu A'^\mu \\ & + \bar{\chi} (i \not{D}_\chi - m_\chi) \chi - \frac{1}{2\xi} (\partial_\mu A'^\mu)^2 \\ & + \frac{1}{2} \partial_\mu \sigma \partial^\mu \sigma - \xi \frac{m_{A'}^2}{2} \sigma^2, \end{aligned} \quad (1)$$

where $m_{A'}$ is the mass of dark photon, χ is a Dirac dark matter field, σ is the singlet Stueckelberg field, ξ is the gauge-fixing parameter. The interaction of dark photon, A'_μ , with charged leptons, ψ_i , can include both diagonal and non-diagonal couplings

$$\mathcal{L}_{A'\psi} = \sum_{i,k=e,\mu,\tau} A'_\mu \bar{\psi}_i \gamma^\mu (g_{ik}^V + g_{ik}^A \gamma_5) \psi_k, \quad (2)$$

where g_{ik}^V and g_{ik}^A are the vector and axial-vector dimensionless couplings, respectively. Such couplings naturally arise in the familion scenarios [14, 15] that imply an ultra-violet completion of the models. The bounds on leptonphilic non-diagonal, $i \neq k$, dark photon couplings in Eq. (2) are derived explicitly in Refs. [14, 15] from anomalous ($g-2$) magnetic moments of charged leptons and the experimental constraints on rare $l_i \rightarrow \gamma l_k$ and $l_i \rightarrow 3 l_k$ decays. It is worth noticing, that diagonal couplings, $i = k$, in Eq. (2) may induce at the one loop level the kinetic mixing between SM photon and dark photon [24] (for a recent review on the corresponding constraints see, e. g., Ref. [6] and references therein).

The paper is organized as follows. In Sec. II we discuss the contribution of dark photon with non-diagonal lepton

*e-mail: zhevlakov@theor.jinr.ru

†e-mail: kirpich@ms2.inr.ac.ru

‡e-mail: valeri.lyubovitskij@uni-tuebingen.de

vertices to the anomalous magnetic moment of leptons. In Sec. III we briefly discuss two body LFV decays involving a sub-GeV vector in the final state, $l_i \rightarrow l_f + A'$. In Sec. IV, we derive the limits for non-diagonal coupling of dark photon from fixed target experiments. Finally, in Sec. V we present our bounds to dark photon non-diagonal couplings with charged leptons and discuss a prospects to search for LFV conversions $eN \rightarrow \mu NA'$, $\mu N \rightarrow e NA'$, $eN \rightarrow \tau NA'$, and $\mu N \rightarrow \tau NA'$ at the fixed target facilities.

II. LEPTON $(g-2)$ TENSIONS

Anomalous magnetic moments of both muon or electron are the quantities that can be used to constrain the parameters of the New physics model. In particular, the current discrepancies of $(g-2)$ quantities for electron and muon between the experimental measurement and theoretical prediction in the framework of SM are

$$\Delta a_\mu = (2.51 \pm 0.59) \times 10^{-9} \quad [1], \quad (3)$$

$$|\Delta a_e| = (4.8 \pm 3.0) \times 10^{-13} \quad [25]. \quad (4)$$

Here we use the difference between theory and experiment for $(g-2)$ of muon based on theoretical analysis from [1]. Now, situation with discrepancy of $(g-2)$ muon is dramatically due to the emergence of new data of two pion contribution to hadronic vacuum polarization (HVP) from CMD-3 Collaboration [26], new measurements of $(g-2)$ from Muon $g-2$ experiment at Fermilab [27] and huge data of new theory discussions about value for HVP term [28–30]. In the BSM framework, the deviation of the magnitudes of muon and electron $(g-2)$ can be potentially explained due to the sub-GeV boson feebly interacting with leptons [31, 32], that implies keeping non-zero diagonal couplings, $g_{ii}^{A,V} \neq 0$, and vanishing of the non-diagonal terms, $g_{ik}^{A,V} \equiv 0$. The precision of the measurements of the tau lepton anomalous magnetic moment is significantly worse, due the lack of experimental data on the short lived tau [33, 34]. For completeness, we

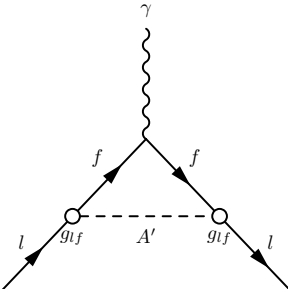


FIG. 1: Diagrams describing the contributions of the dark photon A' to the anomalous magnetic moments δa_l of the leptons with taking into account flavor non-diagonal ($l \neq f$) couplings, where $l, f = e, \mu, \tau$.

cite Ref. [1] for current status of the $(g-2)$ muon puzzle not implying the BSM interpretation.

For the case of finite non-diagonal couplings, $g_{ik}^{A,V} \neq 0$, and vanished $g_{ii}^{V,A} \equiv 0$, the typical contribution of a massive neutral dark vector boson to $(g-2)$ was calculated explicitly in Ref. [15]. In Fig. 1 we show the corresponding one-loop diagram. These quantities are given by one-dimensional integrals over Feynman parameter:

$$\delta a_l^V = \frac{(g_{lf}^V)^2}{4\pi^2} y_l \int_0^1 dx \frac{1-x}{\Delta(x, y_A, y_l)} \left[x \left(2 - y_l(1+x) \right) + \frac{(1-y_l)^2}{2y_A^2} (1+y_l x)(1-x) \right], \quad (5)$$

$$\delta a_l^A = -\frac{(g_{lf}^A)^2}{4\pi^2} y_l \int_0^1 dx \frac{1-x}{\Delta(x, y_A, y_l)} \left[x \left(2 + y_l(1+x) \right) + \frac{(1+y_l)^2}{2y_A^2} (1-y_l x)(1-x) \right], \quad (6)$$

where we use the following notations: $y_l = m_l/m_f$, $y_A = m_{A'}/m_f$ and $\Delta(x, a, b) = a^2 x + (1-x)(1-b^2 x)$, m_l is mass of external lepton, m_f is mass of internal lepton in loop. In Fig. 2 we show the typical bounds on the non-diagonal coupling $g_{\mu e}^V$ from $(g-2)_e$ using a set of the ratios $g_{\mu e}^A/g_{\mu e}^V$. Similar bounds we can obtain from $(g-2)_\mu$ discrepancy for $g_{\mu\tau}^V$ (see details in Ref.[15]).

The most stringent constraint on $g_{\mu e}^V$ implies $g_{\mu e}^A \ll 10^{-8}$, since the typical contributions of vector and axial-vector mediators have an opposite signs in Eqs. (5) and (6) and thus contribution of vector field is maximal. For the benchmark ratio $g_{\mu e}^V \simeq g_{\mu e}^A$ the vector and axial-vector terms almost compensate each other at $m_{A'} \lesssim 2m_\mu$, which leads to a weakening of the limit on $g_{\mu e}^V$. Remarkably, there is a typical sensitivity mass threshold at $m_{A'} \gtrsim 2m_\mu$ for the benchmark ratio $g_{\mu e}^A/g_{\mu e}^V \simeq 1$.

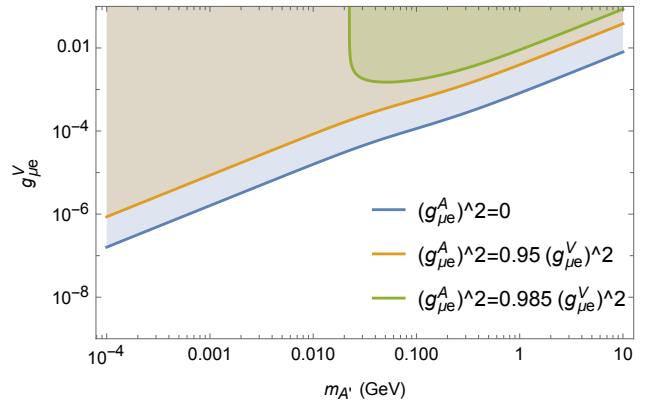


FIG. 2: Bounds for a non-diagonal coupling $g_{\mu e}^V$ from $(g-2)_e$ at different ratio between axial-vector $g_{\mu e}^A$ and vector coupling $g_{\mu e}^V$ of dark photon interaction with muon and electron.

III. INVISIBLE LEPTON DECAY MODE

If dark photon with non-diagonal LFV couplings to muons (tau) and electrons (muon) is relatively light, i. e. $m_i \gtrsim m_{A'} + m_f$, then the decays $\mu \rightarrow e + \text{inv.}$, $\tau \rightarrow e + \text{inv.}$, and $\tau \rightarrow \mu + \text{inv.}$ are kinematically allowed, where we imply the invisible decay of dark photon in the final state $A' \rightarrow \chi\bar{\chi}$. In addition, the typical invisible charged LFV decays are searched in the processes with lepton flavor conversion accompanied by production of pair of neutrino and anti-neutrino [35, 36]. It is worth noticing that the fixed target experiments with missing energy/momenta technique can be a suitable tool to search for them.

The strongest bounds on non-diagonal couplings of dark photon with leptons for area of $m_{A'} < 2m_e$ are obtained from experimental searches for the decays $\tau \rightarrow \mu + \text{inv.}$ and $\tau \rightarrow e + \text{inv.}$ by the ARGUS Collaboration [36], and recent data from the Belle-II Collaboration [37]. We use the PDG data [34] to constrain the non-diagonal dark photon-lepton couplings $g_{\tau e}^{V,A}$ and $g_{\tau \mu}^{V,A}$. For axion-like particles (ALPs) the bounds were obtained in Ref. [38]. For $\mu \rightarrow e + \text{inv.}$ decay we can use the limit obtained by the TWIST Collaboration [35] predicts branching ratio at level up to 5.8×10^{-5} . Using this constraint, we show exclusion plots in Figs. 8 and 9.

Decay widths of such rare charged LFV decays $l_i \rightarrow l_f + A'$ in vector and axial-vector cases are defined as

$$\Gamma(l_i \rightarrow l_f + A')_{V/A} = \frac{3(g_{if}^{V/A})^2 m_i}{8\pi} \lambda^{1/2}(y_i^2, y_f^2, 1) \times \left[(y_i \mp y_f)^2 - 1 + \frac{y_i^2}{3} \lambda(y_i^2, y_f^2, 1) \right], \quad (7)$$

where $y_i = m_i/m_{A'}$, $y_f = m_f/m_{A'}$, and $\lambda(x, y, z) = x^2 + y^2 + z^2 - 2xy - 2xz - 2yz$ is the Källen kinematical triangle function.

It is important to note that this decay depends only on non-diagonal coupling, while other LFV lepton decays as $l_i \rightarrow l_f + \gamma$ or $l_i \rightarrow 3l_f$ have a dependence from the product of diagonal and non-diagonal couplings. Analysis of the parameter space of dark photon was done in Ref. [39] where implication of the charged LFV two body decay has been noted.

IV. THE FIXED-TARGET EXPERIMENTS

Fixed target experiments represent themselves very useful and crucial test of physics of feebly interacting particles and make up a third of the experimental base for searching and analysis of DM [40] or hidden sector. In this section we study dark photon emission reactions with change of lepton flavor.

In the framework of the benchmark scenario (2), stringent limits can be established from the missing energy/momenta experiments by analysis of $l_i + N \rightarrow$

$l_f + N + A'$ process. In particular, we will discuss the potential for the fixed target experiments with lepton beams such as NA64e [32, 41–45], LDMX [46–50], NA64 μ [51–54] and M³ [55, 56], which can be used to probe the invisible signatures associated with a lepton flavor violation and missing energy process. Missing energy signals can be evidence of dark photon emission that involves LFV processes. Analysis of final lepton states can give information about specific LFV channels of lepton conversion with dark photon emission.

The existed (NA64e [32, 41–45] and NA64 μ [51–54]) and future experiments (LDMX [46–50], M³ [55, 56]) are noted by us due to a possibility of using missing energy/momentum technique. Experiments NA64 e and LDMX use electron beams which collide to active lead and aluminium targets, respectively. Experiments NA64 μ and M³ use muon beams, M³ will use tungsten target. We collect the main parameters of the fixed-target experiments NA64 e , NA64 μ , M³, and LDMX in Table I.

It is worth noticing that analysis of LFV with dark matter emission at fixed-target experiments was done for the scalar case. In this respect we can mention Refs. [8, 57, 58] that examine the invisible scalar portal scenarios. A possibility of $e - \tau$ and $\mu - \tau$ conversion in deep-inelastic lepton scattering off nuclei was proposed and studied in detail in Ref. [59] based on assumption of local four-fermion lepton-quark interaction. Besides, huge research lepton conversion on nucleons was made in Refs.[60–63].

A. Signal of lepton conversion

Based on the setup of the missing energy experiment we will consider the reaction of lepton scattering off the nucleus target as shown in Fig. 3. We propose that dark photon have a lifetime larger than time of flight inside the detector or dominant decay mode into dark matter. The invisible two-body decay width of dark photon A' into $\chi\bar{\chi}$ pair is given by

$$\Gamma_{A' \rightarrow \chi\bar{\chi}} = \frac{g_D^2}{12\pi} m_{A'} (1 + 2y_\chi^2) (1 - 4y_\chi^2)^{1/2}. \quad (8)$$

where g_D is coupling dark photon with dark fermions and $y_\chi = m_\chi/m_{A'}$.

For calculation we will use Weizsäcker-Williams (WW) approximation [64, 65]. In this case, the signal of interaction of incoming leptons (e, μ) with atomic target can be effectively described through the Compton-like conversion on virtual photons γ^* , i. e. via $l\gamma^* \rightarrow l'A'$. We also suppose that target nucleus has a spin=1/2 and its coupling to photon is $ieZF(t)\gamma_\mu$, where $F(t)$ is an elastic form factor depending on $t = -q^2 > 0$ (nucleus transfer momentum squared), Z is the charge of nucleus. $F(t)$ has the form

$$F(t) = \frac{a^2 t}{(1 + a^2 t)} \frac{1}{(1 + t/d)}, \quad (9)$$

TABLE I: Parameters of the fixed-target experiments NA64_e, NA64_μ, M³, and LDMX: parameters of target (A, Z), first radiation length X_0 , effective thickness of the target (L_T), energy of scattering beam and current (started) and planned accumulate of leptons on target, x_{min} characterizing a window of search.

	e -conv.	μ -conv.	A (Z)	E (GeV)	ρ (g cm ⁻³)	X_0 (cm)	L_T (cm)	x_{min}	LoT (projected LoT)
NA64 _e : $eN \rightarrow NA'\mu(\tau)$	—	—	207 (82)	100	11.34	0.56	0.56	0.5	3.3×10^{11} (5×10^{12})
NA64 _μ :	—	$\mu N \rightarrow NA'e(\tau)$	207 (82)	160	11.34	0.56	22.5	0.5	10^{10} (10^{13})
M ³ :	—	$\mu N \rightarrow NA'e(\tau)$	184 (74)	15	19.3	0.35	17.5	0.4	10^{10} (10^{13})
LDMX: $eN \rightarrow NA'\mu(\tau)$	—	—	27 (13)	16	2.7	8.9	3.56	0.7	10^{16} (10^{18})

where $a = 111Z^{-1/3}/m_e$ and $d = 0.164A^{-2/3}$ GeV² are the screening and nucleus size parameters, respectively [66]. These parameters of nuclear form factor include m_e which is mass of electron and A is atomic weight number.

Differential cross section for $2 \rightarrow 3$ process, presented in Fig. 3, in the framework of the WW approximation is given by

$$\frac{d\sigma_{lZ \rightarrow l'ZA'}}{d(pk)d(k\mathcal{P}_i)} \simeq \frac{\alpha\gamma_Z}{\pi(p'\mathcal{P}_i)} \cdot \frac{d\sigma_{l\gamma^* \rightarrow l'A'}}{d(pk)} \Big|_{t=t_{min}}, \quad (10)$$

where t_{min} is a minimal momentum transfer that is provided below in Eq. (19), $\alpha \simeq 1/137.036$ is a fine structure constant, γ_Z is the effective photon flux from nucleus defined as

$$\gamma_Z = Z^2 \int_{t_{min}}^{t_{max}} dt \frac{t - t_{min}}{t^2} F^2(t). \quad (11)$$

where \mathcal{P}_i is momentum of nuclear, p, p' and k are momenta of initial, finale leptons and dark photon (see definition in Fig. 3), t_{max} and t_{min} are kinematic bounds is obtained from the energy-conserving δ -function in the Lorentz-invariant phase space (details in Ref.[67]).

By using such approximation, we can calculate the typical number of missing energy events for experiments with lepton beam impinging on the fixed target

$$N_{A'} \simeq \text{LoT} \cdot \frac{\rho N_A}{A} L_T \int_{x_{min}}^{x_{max}} dx \frac{d\sigma_{2 \rightarrow 3}(E)}{dx}, \quad (12)$$

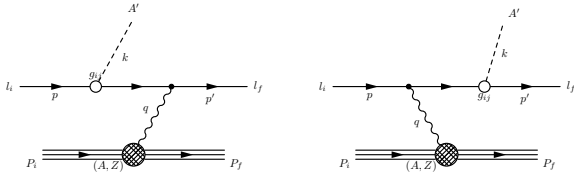


FIG. 3: Lowest-order diagrams describing LFV emission of dark photon A' in lepton scattering on fixed atomic target.

where N_A is the Avogadro's number, LoT is number of leptons accumulated on target, ρ is the target density, L_T is the effective interaction length of the lepton in the target, $d\sigma_{2 \rightarrow 3}/dx$ is the differential cross section of the lepton conversion $lN \rightarrow l'NA'$, E is a initial lepton beam energy, $x = E_{A'}/E$ is the energy fraction that dark photon carries away, $x_{min} = E_{cut}/E$ and $x_{max} \simeq 1$ are the minimal and maximal fraction of dark photon energy respectively for the regarding experimental setup, E_{cut} is a detector missing energy cut that is determined by the specific facility. The typical parameters of the experiments can be found in Refs. [32, 41–44, 46–50, 53–56, 68]. For muon beam experiments (NA64_μ and M³) we will used definition MoT for number of muons on target, for electron beam experiments (NA64_e and LDMX) will be used EoT for number of electrons on target. There are the parameters determined by technical characteristics of detectors and by background cutoff.

B. Cross-section

Amplitude of the $2 \rightarrow 2$ process $l_i(p) + \gamma(q) \rightarrow l_f(p') + A'(k)$ is given by

$$M^{2 \rightarrow 2} = ie \epsilon_\lambda^\mu \epsilon_{\lambda'}^{\alpha\nu} \bar{u}_f(p', s') \left[\gamma_\mu \frac{\not{p} - \not{k} + m_i}{\tilde{u}} (\gamma_\alpha g_{if}^V + \gamma_5 \gamma_\alpha g_{if}^A) + (\gamma_\alpha g_{if}^V + \gamma_5 \gamma_\alpha g_{if}^A) \frac{\not{p}' + \not{k} + m_f}{\tilde{s}} \gamma_\mu \right] u_i(p, s), \quad (13)$$

where used notation $\not{p} = \gamma^\mu p_\mu$, g_{if}^V and g_{if}^A are the non-diagonal couplings of interaction of dark photon with leptons, ϵ is the polarization vector of photon or dark photon, m_i and m_f are the masses of initial and final leptons. The sums over polarizations are given by

$$\sum_\lambda \epsilon_\lambda^\mu \epsilon_{\lambda'}^{\alpha\nu} = -g^{\mu\nu}, \quad (14)$$

for visible photon and

$$\sum_{\lambda'} \epsilon_{\lambda'}^\mu \epsilon_{\lambda'}^{\alpha\nu} = -g^{\mu\nu} + \frac{k^\mu k^\nu}{m_{A'}^2}, \quad (15)$$

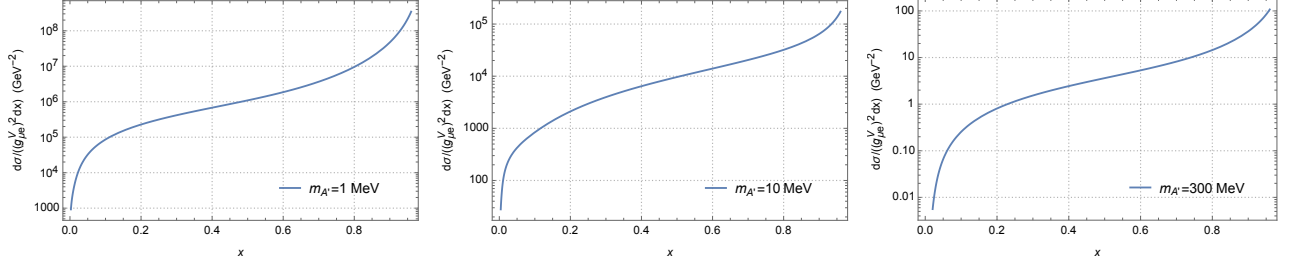


FIG. 4: Differential cross section $d\sigma/((g_{\mu e}^V)^2 dx)$ for the process of electron to muon conversion in the case of vector non-diagonal coupling of dark photon with lepton for the NA64e experiment with different masses of dark photon and the typical energy of electron beam $E = 100$ GeV.

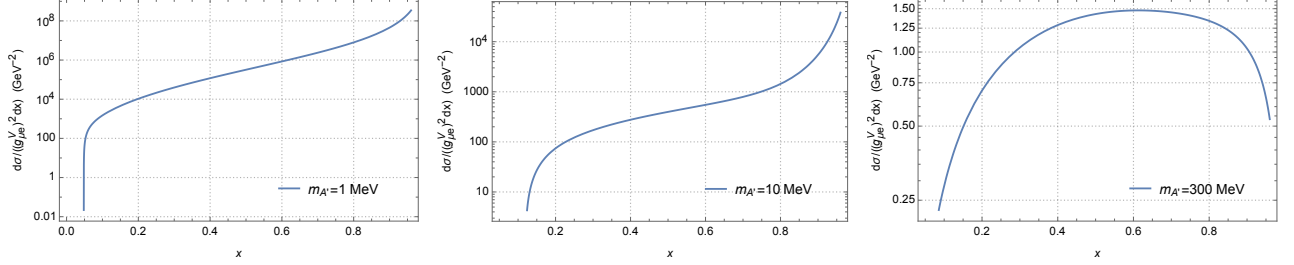


FIG. 5: Differential cross section $d\sigma/((g_{\mu e}^V)^2 dx)$ for the process of muon to electron conversion in the case of vector non-diagonal coupling of dark photon with lepton for the NA64 μ experiment with different masses of dark photon and the typical energy of muon beam $E = 160$ GeV.

for massive dark photon. In case of visible photon we use $\xi \rightarrow \infty$ gauge omitting ghost fields contribution.

After averaging and summation over spins of leptons and polarizations of vector bosons one gets the matrix element squared

$$\begin{aligned} \overline{|M^{2 \rightarrow 2}|^2} &= \frac{1}{4} \sum_{s, s'} \sum_{\lambda, \lambda'} |M^{2 \rightarrow 2}|^2 \\ &= e^2 (g_{if}^V)^2 A_V^{2 \rightarrow 2} + e^2 (g_{if}^A)^2 A_A^{2 \rightarrow 2}. \end{aligned} \quad (16)$$

In our calculation we will use the so-called modified Mandelstam variables:

$$\begin{aligned} \tilde{s} &= (p' + k)^2 - m_f^2 = 2(p'k) + m_{A'}^2, \\ \tilde{u} &= (p - k)^2 - m_i^2 = -2(pk) + m_{A'}^2, \\ t_2 &= (p' - p)^2 = -2(p'p) + m_i^2 + m_f^2, \\ t &= q^2, \end{aligned} \quad (17)$$

which satisfy the condition $\tilde{s} + t_2 + \tilde{u} = m_{A'}^2$.

When considering the process, we have an energy of initial lepton energy much greater than masses of $m_{A'}$ and m_f . In this case we can use WW approximation and can propose with high reliability that the final state of lepton and dark photon are highly collinear. When, in the small-angle approximation (which means that $t = t_{min}$) we imply that \mathbf{q} and $\mathbf{V} = \mathbf{k} - \mathbf{p}$ are collinear [65, 67]

and the modified Mandelstam variables are given by

$$\begin{aligned} U = -\tilde{u} &\approx E^2 x \theta^2 + m_i^2 x + \frac{1-x}{x} m_{A'}^2, \\ \tilde{s} &\approx \frac{U + (m_f^2 - m_i^2)x}{1-x}, \end{aligned} \quad (18)$$

$$\begin{aligned} t_2 &\approx -\frac{x}{1-x} (U + (m_f^2 - m_i^2)) + m_{A'}^2, \\ t_{min} &\approx \frac{(\tilde{s} + (m_f^2 - m_i^2))^2}{4E^2}. \end{aligned} \quad (19)$$

Note that if we set $m_i = m_f$, then we reproduce formulas presented in Ref. [66, 67].

The double differential cross-section can be presented in the form

$$\frac{d\sigma_{2 \rightarrow 3}}{dx d\cos\theta_{A'}} \simeq \frac{\alpha\gamma_Z}{\pi(1-x)} \cdot E^2 x \beta_{A'} I_{\tilde{s}} \cdot \frac{d\sigma_{2 \rightarrow 2}}{d(pk)}, \quad (20)$$

where $\beta_{A'} = (1 - m_{A'}^2/(xE)^2)^{1/2}$ is the velocity of dark photon in the laboratory frame, $I_{\tilde{s}} = \tilde{s}^2/(\tilde{s} + (m_f^2 - m_i^2))^2 \beta_{m_i}^{-1}$, $\beta_{m_i} = \sqrt{1 - m_i^2/E^2}$. Full analytical expression for the effective photon flux χ is presented in the Ref. [53]. It is known that the elastic form-factor $G_{el}(t)$ is proportional to $\propto Z^2$. An inelastic form-factor is suppressed by a factor Z , i.e. $G_{inel}(t) \propto Z$, and therefore for the heavy target nuclei $Z \propto \mathcal{O}(100)$ one can safely ignore it in calculation.

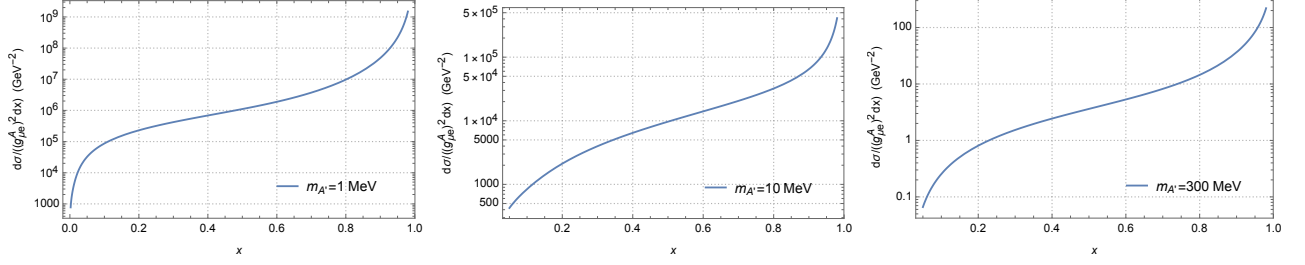


FIG. 6: The same as in Fig. 4 but for axial vector field.

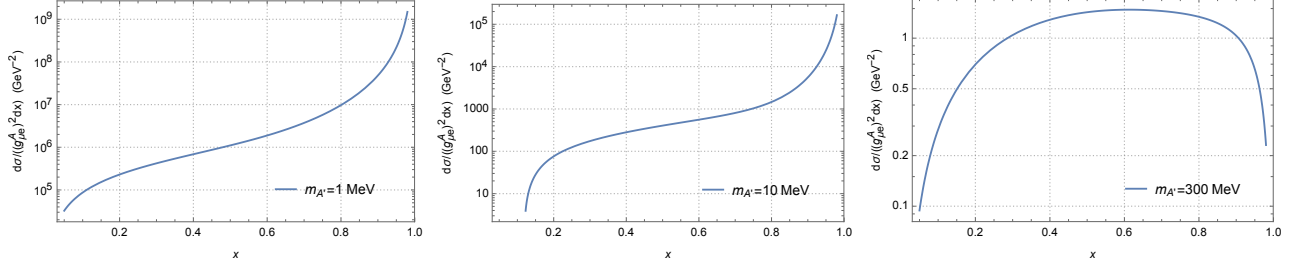


FIG. 7: The same as in Fig. 5 but for axial vector field.

Differential cross section [67] can be rewritten as

$$\frac{d\sigma_{2 \rightarrow 2}^{V,A}}{d(pk)} = 2 \frac{d\sigma}{dt_2} = \frac{|\overline{M^{2 \rightarrow 2}}|^2}{8\pi \tilde{s}^2} = (g_{if}^{V,A})^2 \frac{\alpha}{\tilde{s}^2} A_{V,A}^{2 \rightarrow 2}, \quad (21)$$

where the vector and axial-vector parts of the amplitudes squared can be written, respectively, as:

$$\begin{aligned} A_{V,t=t_{\min}}^{2 \rightarrow 2} \approx & \frac{1}{\tilde{s}^2 U^2 m_{A'}^2} \left(\tilde{s}(\tilde{s} - U)^2 U (m_i - m_f)^2 + (2\tilde{s}U(\tilde{s}^2 + U^2) + (\tilde{s}^2 + U^2)m_i^4 + 6(\tilde{s} - U)^2 m_i^3 m_f + \right. \\ & + 2(\tilde{s}^3 + 2\tilde{s}^2 U + U^3)m_f^2 + (\tilde{s}^2 + U^2)m_f^4 + 6m_i m_f (U - \tilde{s})(2\tilde{s}U + (U - \tilde{s})m_f^2) \\ & - 2m_i^2(\tilde{s}^3 + 2\tilde{s}U^2 + U^3 + (3\tilde{s}^2 - 4\tilde{s}U + 3U^2)m_f^2))m_{A'}^2 + 2(2\tilde{s}U(U - \tilde{s}) + U(-3\tilde{s} + 2U)m_i^2 + \\ & \left. + 6\tilde{s}U m_i m_f + \tilde{s}(2\tilde{s} - 3U)m_f^2)m_{A'}^4 + 4\tilde{s}U m_{A'}^6 \right), \end{aligned} \quad (22)$$

$$\begin{aligned} A_{A,t=t_{\min}}^{2 \rightarrow 2} \approx & \frac{1}{\tilde{s}^2 U^2 m_{A'}^2} \left(\tilde{s}(\tilde{s} - U)^2 U (m_i + m_f)^2 + (2\tilde{s}U(\tilde{s}^2 + U^2) + (\tilde{s}^2 + U^2)m_i^4 - 6(\tilde{s} - U)^2 m_i^3 m_f \right. \\ & + 2(\tilde{s}^3 + 2\tilde{s}^2 U + U^3)m_f^2 + (\tilde{s}^2 + U^2)m_f^4 + 6(U - \tilde{s})m_i m_f (-2\tilde{s}U + (\tilde{s} - U)m_f^2) \\ & - 2m_i^2(\tilde{s}^3 + 2\tilde{s}U^2 + U^3 + (3\tilde{s}^2 - 4\tilde{s}U + 3U^2)m_f^2))m_{A'}^2 - 2(2\tilde{s}(\tilde{s} - U)U + (3\tilde{s} - 2U)U m_i^2 \\ & \left. + 6\tilde{s}U m_i m_f + \tilde{s}(3U - 2\tilde{s})m_f^2)m_{A'}^4 + 4\tilde{s}U m_{A'}^6 \right). \end{aligned} \quad (23)$$

In our calculations we used the FeynCalc package [69–71] and the following assumptions to exploit the WW approximation: (i) cross section for processes with $m_i > m_f$ was evaluated by taking into account non-zero emission angle of the final particle [72]: $\theta_{\min} \simeq [(m_i^2 + m_{A'}^2 -$

$m_f^2)/(|\mathbf{k}||\mathbf{p}|)]^{1/2}$, (ii) the maximal typical angle of dark photon emission was set to be $\theta_{\max} \simeq 0.1$. As a result, the integration over the angle $\theta_{A'}$ is performed in the range $\theta_{\min} \lesssim \theta_{A'} \lesssim \theta_{\max}$.

In order to illustrate our results for the differential

cross sections $d\sigma/dx$ we make a comparison for different combinations of initial and final states of leptons. In particular, we demonstrate it in Figs. 4-7. For the case of equal masses of initial and final leptons we reproduce the numerical results presented in Refs. [31, 67]. These cross sections $d\sigma/dx$ are calculated by using Eqs. (20) and (21) implying the lepton beam energy and target characteristics of the NA64e and NA64 $_{\mu}$ experiments. One can see the similar shapes of the vector and axial-vector dark photon in case of $e \rightarrow \mu$ conversion cross sections at $m_{A'} \simeq 1$ MeV. For larger masses $m_{A'} \gtrsim 300$ MeV the differential spectra of vector and axial vector are almost coincided. For the case of $\mu \rightarrow e$ conversion cross sections one can see there are sharp peaks at $x \simeq 1$ for the relatively light dark photon $m_{A'} \lesssim 10$ MeV. The corresponding peaks are mitigated for heavy masses $m_{A'} \gtrsim 300$ MeV.

V. RESULTS AND DISCUSSION

In this section we derived the bounds on non-diagonal $g_{ik}^{V,A}$ couplings of dark photon with leptons from the lepton scattering experiments at fixed targets, that implies LFV conversion $lN \rightarrow l'NA'$ followed by the invisible decay of dark photon with $\text{Br}(A' \rightarrow \chi\bar{\chi}) \simeq 1$. We set the diagonal couplings to be $g_{ii}^{V,A} \equiv 0$ throughout the analysis.

Our results for exclusion limits on vector and axial-vector couplings are presented in Fig. 8 and Fig. 9 at 90 % C.L., implying zero observed signal events and background free case and null-result of the fixed target experiments and on assumption that theoretical uncertainty is negligible, $N_{A'} \lesssim 2.3$. In particular, the analysis reveals [73] that the electron beam mode NA64 $_e$ is background free for $\text{EoT} \simeq \mathcal{O}(1) \times 10^{12}$. In addition, for our analysis of the muon beam mode at NA64 $_{\mu}$ we rely on the study [54, 57, 74] that implies the background suppression at the level of $\lesssim \mathcal{O}(1) \times 10^{-13}$ per muon for the LFV process due to the emission of spin-0 boson ϕ , i. e. in the reaction $lN \rightarrow l'N\phi$. Furthermore, for the background suppression of both LDMX and M^3 facilities we rely on the explicit analysis of [75] and [55] respectively for the reactions without LFV, $lN \rightarrow l'NA'$, implying conservatively that the regarding background rejections would be the same for LFV process, $lN \rightarrow l'NA'$.

To search for a channel of LFV conversion in $lN \rightarrow l'NA'$ process is needed to search a signal with missing energy and single different flavor lepton. For the benchmark conversion $e(\mu)N \rightarrow \tau NA'$ and the typical dark photon mass range $m_{A'} \lesssim 1$ GeV, the existing fixed-target experiments (NA64 $_e$ and NA64 $_{\mu}$) can not reach the bound on $\tau \rightarrow e(\mu)A'$ from ARGUS experiment [36] for both vector $g_{e\tau}^V$ and axial-vector $g_{e\tau}^A$ couplings. For the considered benchmark scenarios, the most stringent constraints on the couplings $g_{e\tau}^V \lesssim 10^{-11}$ and

$g_{e\tau}^A \lesssim 10^{-11}$ at $m_{A'} \lesssim 1$ MeV are expected from the projected statistics ($\text{EoT} = 10^{18}$) of the LDMX experiment. However, for the typical mass range $m_{A'} \gtrsim 100$ MeV the LDMX is able to set the constraint at the level of $g_{\mu e}^{V,A} \lesssim 10^{-7}$. Remarkably, for the typical mass range $m_{A'} \gtrsim m_{\tau} \simeq 1.7$ GeV, the LDMX facility can set the

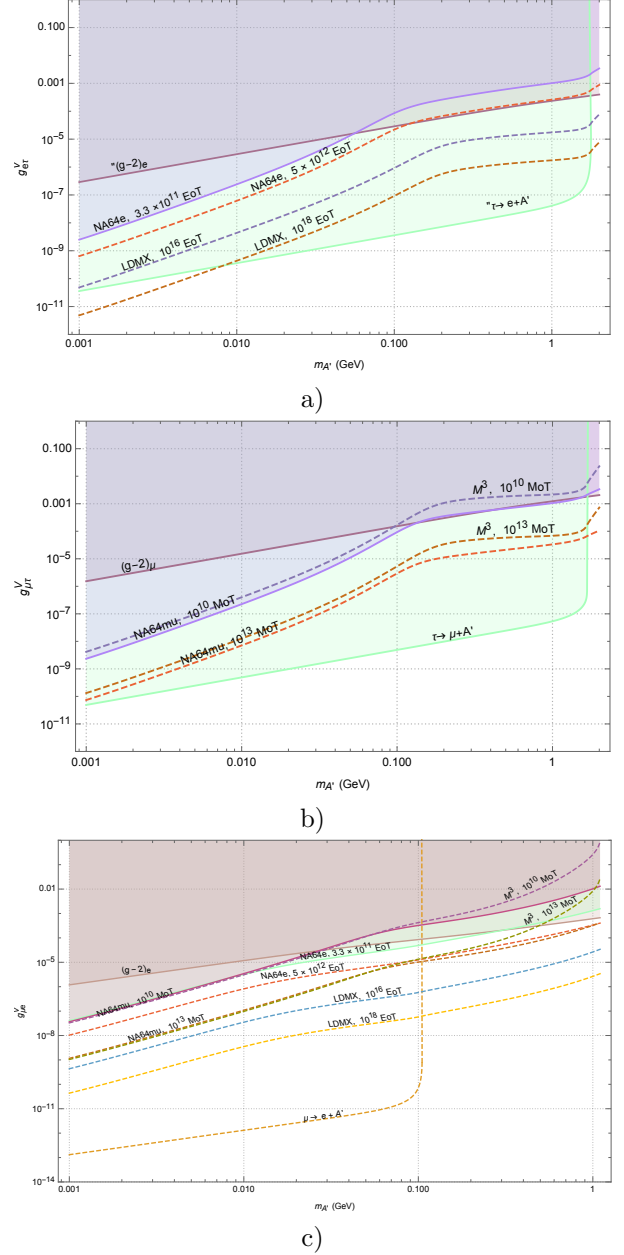


FIG. 8: Bounds on vector non-diagonal coupling of dark photon with leptons using characteristics of running and proposed fixed-target experiments NA64 $_e$, NA64 $_{\mu}$, LDMX, and M^3 . Bounds from $g-2$ of leptons and invisible lepton LFV decay $l_i \rightarrow l_f + A'$ are included. Panel (a): bounds for $g_{e\tau}^V$, panel (b): bounds for $g_{\mu\tau}^V$, panel (c): bounds for $g_{\mu e}^V$.

bounds at $g_{e\tau}^{V,A} \lesssim 10^{-5} - 10^{-4}$. For the accumulated statistics of NA64_e at the level of EoT $\simeq 3.3 \times 10^{11}$ the corresponding experiment provides the bound $g_{e\tau}^A \lesssim 5 \times 10^{-3}$ for the mass threshold range $m_{A'} \gtrsim 1.7$ GeV. In addition, the NA64_e also rules out the typical regions $g_{\mu e}^V \lesssim 10^{-4}$ for $100 \text{ MeV} \lesssim m_{A'} \lesssim 300 \text{ MeV}$ and $g_{\mu e}^A \lesssim 10^{-3} - 10^{-2}$ for $100 \text{ MeV} \lesssim m_{A'} \lesssim 1 \text{ GeV}$.

The NA64_μ fixed target experiment can provide a more stringent limit than the M³ facility. Moreover, the expected reaches of the LDMX and NA64_μ experiments at the masses of dark photon $m_{A'} \lesssim 1 \text{ MeV}$ can be comparable with the current bounds from two-body LFV lepton decay, $\tau \rightarrow \mu(e)A'$. In addition, the current limits from missing energy data of the NA64_e and NA64_μ experiments are comparable with the bounds from $(g-2)_{e,\mu}$ tensions of leptons. We note that for the projected statistics MoT $\simeq 10^{13}$ both NA64_μ and M³ can rule out the typical region $g_{\mu\tau}^{V,A} \lesssim 10^{-4} - 10^{-3}$ for the relatively heavy masses of dark photon $m_{A'} \gtrsim 1.7 \text{ GeV}$. Moreover, for the mass range $100 \text{ MeV} \lesssim m_{A'} \lesssim 1 \text{ GeV}$ the NA64_μ is able to set the constraint $g_{\mu e}^{A,V} \lesssim 10^{-5}$ for MoT $\simeq 10^{13}$.

Finally, we would like to note that one can probe the

resonant production of dark photons in the LFV reaction of muon scattering off atomic electrons $\mu^+e^- \rightarrow A' \rightarrow \chi\bar{\chi}$ at both NA64_μ and M³ muon beam fixed target experiments. However, this analysis is beyond the scope of the present paper and we plan to study it in future.

Acknowledgments

The work of A. S. Zh. on exclusion limits calculation for the fixed target experiments is supported by Russian Science Foundation (grant No. RSF 23-22-00041). The work of A. S. Zh. on exclusion limit calculation from $(g-2)$ tension is supported by the Foundation for the Advancement of Theoretical Physics and Mathematics "BASIS". The work of D. V. K. on signal yield calculation for the $e \rightarrow \mu$ conversion at NA64_e experiments is supported by the Russian Science Foundation (grant No. RSF 21-12-00379). The work of V. E. L. was funded by ANID PIA/APOYO AFB220004 (Chile), by FONDECYT (Chile) under Grant No. 1230160, and by ANID–Millennium Program–ICN2019_044 (Chile).

-
- [1] T. Aoyama et al., Phys. Rept. **887**, 1 (2020), 2006.04822.
 - [2] E. Aprile et al. (XENON Collaboration), Phys. Rev. D **102**, 072004 (2020), 2006.09721.
 - [3] T. Aaltonen et al. (CDF Collaboration), Science **376**, 170 (2022).
 - [4] A. A. Aguilar-Arevalo et al. (MiniBooNE Collaboration), Phys. Rev. D **103**, 052002 (2021), 2006.16883.
 - [5] A. J. Krasznahorkay et al., Phys. Rev. Lett. **116**, 042501 (2016), 1504.01527.
 - [6] C. Antel et al., in *Workshop on Feebly-Interacting Particles* (2023), 2305.01715.
 - [7] G. Arcadi, A. Djouadi, and M. Raidal, Phys. Rept. **842**, 1 (2020), 1903.03616.
 - [8] S. N. Gninenko and N. V. Krasnikov, Phys. Rev. D **106**, 015003 (2022), 2202.04410.
 - [9] H. Davoudiasl, R. Marcarelli, and E. T. Neil, JHEP **02**, 071 (2023), 2112.04513.
 - [10] I. V. Voronchikhin and D. V. Kirpichnikov, Phys. Rev. D **107**, 115034 (2023), 2304.14052.
 - [11] I. V. Voronchikhin and D. V. Kirpichnikov, Phys. Rev. D **106**, 115041 (2022), 2210.00751.
 - [12] Y.-J. Kang and H. M. Lee, Eur. Phys. J. C **80**, 602 (2020), 2001.04868.
 - [13] F. Fortuna, P. Roig, and J. Wudka, JHEP **02**, 223 (2021), 2008.10609.
 - [14] A. J. Buras, A. Crivellin, F. Kirk, C. A. Manzari, and M. Montull, JHEP **06**, 068 (2021), 2104.07680.
 - [15] A. Kachanovich, S. Kovalenko, S. Kuleshov, V. E. Lyubovitskij, and A. S. Zhevlakov, Phys. Rev. D **105**, 075004 (2022), 2111.12522.
 - [16] M. Escudero, N. Rius, and V. Sanz, JHEP **02**, 045 (2017), 1606.01258.
 - [17] Y. Nomura and J. Thaler, Phys. Rev. D **79**, 075008 (2009), 0810.5397.
 - [18] V. E. Lyubovitskij, A. S. Zhevlakov, A. Kachanovich, and S. Kuleshov, Phys. Rev. D **107**, 055006 (2023), 2210.05555.
 - [19] G. Arcadi, C. P. Ferreira, F. Goertz, M. M. Guzzo, F. S. Queiroz, and A. C. O. Santos, Phys. Rev. D **97**, 075022 (2018), 1712.02373.
 - [20] C. Han, M. L. López-Ibañez, A. Melis, O. Vives, and J. M. Yang, Phys. Rev. D **103**, 035028 (2021), 2007.08834.
 - [21] D. Aloni, A. Dery, C. Frugiuele, and Y. Nir, JHEP **11**, 109 (2017), 1708.06161.
 - [22] Z. Poh and S. Raby, Phys. Rev. D **96**, 015032 (2017), 1705.07007.
 - [23] T. Araki, K. Asai, H. Otono, T. Shimomura, and Y. Takubo, JHEP **01**, 145 (2023), 2210.12730.
 - [24] B. Holdom, Phys. Lett. B **166**, 196 (1986).
 - [25] L. Morel, Z. Yao, P. Cladé, and S. Guellati-Khélifa, Nature **588**, 61 (2020).
 - [26] F. V. Ignatov et al. (CMD-3) (2023), 2302.08834.
 - [27] D. P. Aguillard et al. (Muon g-2), Phys. Rev. Lett. **131**, 161802 (2023), 2308.06230.
 - [28] T. Blum et al. (RBC, UKQCD), Phys. Rev. D **108**, 054507 (2023), 2301.08696.
 - [29] M. Davier, A. Hoecker, A. M. Lutz, B. Malaescu, and Z. Zhang (2023), 2312.02053.
 - [30] S. Borsanyi et al., Nature **593**, 51 (2021), 2002.12347.
 - [31] D. V. Kirpichnikov, V. E. Lyubovitskij, and A. S. Zhevlakov, Phys. Rev. D **102**, 095024 (2020), 2002.07496.
 - [32] Y. M. Andreev et al. (NA64 Collaboration), Phys. Rev. Lett. **126**, 211802 (2021), 2102.01885.
 - [33] S. Eidelman and M. Passera, Mod. Phys. Lett. A **22**, 159 (2007), hep-ph/0701260.
 - [34] R. L. Workman et al. (Particle Data Group), PTEP **2022**, 083C01 (2022).
 - [35] R. Bayes et al. (TWIST Collaboration), Phys. Rev. D **91**, 052020 (2015), 1409.0638.

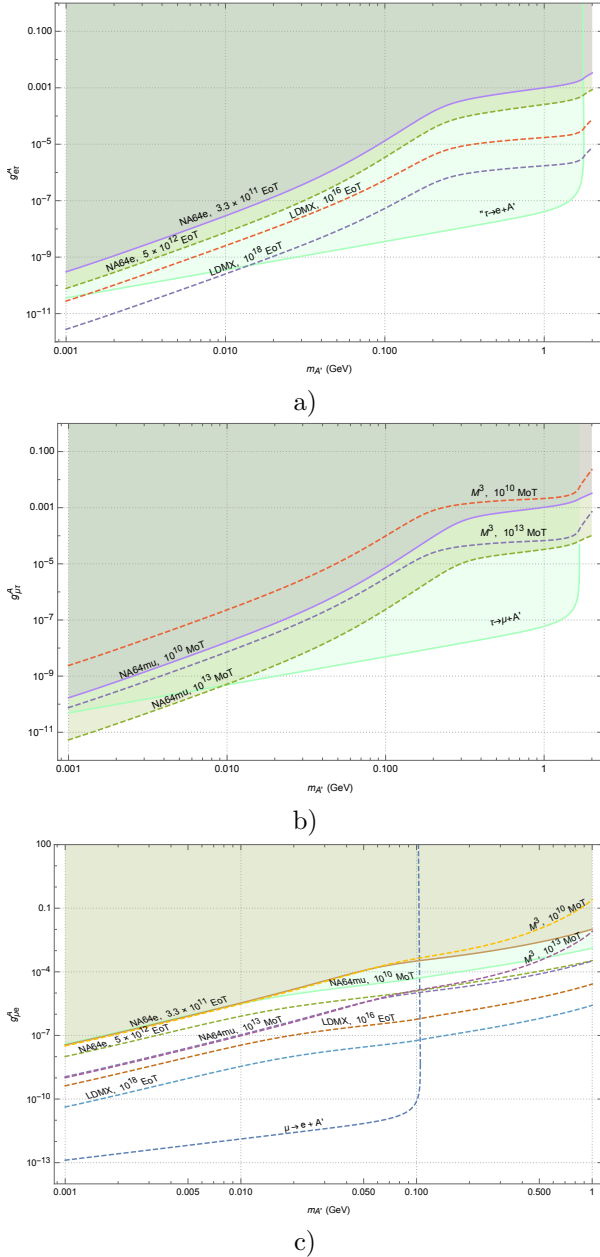


FIG. 9: Bounds axial-vector for non-diagonal coupling interaction of dark photon with leptons using current and proposal experimental characteristics of fix target experiments NA64e, NA64 μ , LDMX and M³. Bounds from $g-2$ of leptons and invisible lepton LFV decay $l_i \rightarrow l_f + A'$ are included. a) Bounds for $g_{e\tau}^A$, b) bounds for $g_{\mu\tau}^A$ and c) bounds for $g_{\mu e}^A$.

[36] H. Albrecht et al. (ARGUS Collaboration), Z. Phys. C **68**, 25 (1995).
 [37] I. Adachi et al. (Belle-II Collaboration), Phys. Rev. Lett. **130**, 181803 (2023), 2212.03634.
 [38] M. Bauer, M. Neubert, S. Renner, M. Schnubel, and A. Thamm, Phys. Rev. Lett. **124**, 211803 (2020),

1908.00008.
 [39] J. Heeck, Phys. Lett. B **758**, 101 (2016), 1602.03810.
 [40] G. Lanfranchi, M. Pospelov, and P. Schuster, Ann. Rev. Nucl. Part. Sci. **71**, 279 (2021), 2011.02157.
 [41] S. N. Gninenko, D. V. Kirpichnikov, M. M. Kirsanov, and N. V. Krasnikov, Phys. Lett. B **782**, 406 (2018), 1712.05706.
 [42] S. N. Gninenko, D. V. Kirpichnikov, M. M. Kirsanov, and N. V. Krasnikov, Phys. Lett. B **796**, 117 (2019), 1903.07899.
 [43] D. Banerjee et al., Phys. Rev. Lett. **123**, 121801 (2019), 1906.00176.
 [44] Y. M. Andreev et al., Phys. Rev. D **104**, L091701 (2021), 2108.04195.
 [45] N. Arefyeva, S. Gninenko, D. Gorbunov, and D. Kirpichnikov, Phys. Rev. D **106**, 035029 (2022), 2204.03984.
 [46] A. Berlin, N. Blinov, G. Krnjaic, P. Schuster, and N. Toro, Phys. Rev. D **99**, 075001 (2019), 1807.01730.
 [47] T. Åkesson et al. (LDMX Collaboration) (2018), 1808.05219.
 [48] A. M. Ankowski, A. Friedland, S. W. Li, O. Moreno, P. Schuster, N. Toro, and N. Tran, Phys. Rev. D **101**, 053004 (2020), 1912.06140.
 [49] P. Schuster, N. Toro, and K. Zhou, Phys. Rev. D **105**, 035036 (2022), 2112.02104.
 [50] T. Åkesson et al., in *Snowmass 2021* (2022), 2203.08192.
 [51] S. N. Gninenko, N. V. Krasnikov, and V. A. Matveev, Phys. Rev. D **91**, 095015 (2015), 1412.1400.
 [52] S. N. Gninenko and N. V. Krasnikov, Phys. Lett. B **783**, 24 (2018), 1801.10448.
 [53] D. V. Kirpichnikov, H. Sieber, L. M. Bueno, P. Crivelli, and M. M. Kirsanov, Phys. Rev. D **104**, 076012 (2021), 2107.13297.
 [54] H. Sieber, D. Banerjee, P. Crivelli, E. Depero, S. N. Gninenko, D. V. Kirpichnikov, M. M. Kirsanov, V. Poliakov, and L. Molina Bueno, Phys. Rev. D **105**, 052006 (2022), 2110.15111.
 [55] Y. Kahn, G. Krnjaic, N. Tran, and A. Whitbeck, JHEP **09**, 153 (2018), 1804.03144.
 [56] R. Capdevilla, D. Curtin, Y. Kahn, and G. Krnjaic, JHEP **04**, 129 (2022), 2112.08377.
 [57] B. Radics, L. Molina-Bueno, L. Fields., H. Sieber, and P. Crivelli, Eur. Phys. J. C **83**, 775 (2023), 2306.07405.
 [58] Y. Ema, Z. Liu, K.-F. Lyu, and M. Pospelov, JHEP **02**, 135 (2023), 2211.00664.
 [59] S. Gninenko, S. Kovalenko, S. Kuleshov, V. E. Lyubovitskij, and A. S. Zhevlakov, Phys. Rev. D **98**, 015007 (2018), 1804.05550.
 [60] M. Gonzalez, T. Gutsche, J. C. Helo, S. Kovalenko, V. E. Lyubovitskij, and I. Schmidt, Phys. Rev. D **87**, 096020 (2013), 1303.0596.
 [61] A. Faessler, T. Gutsche, S. Kovalenko, V. E. Lyubovitskij, and I. Schmidt, Phys. Rev. D **72**, 075006 (2005), hep-ph/0507033.
 [62] A. Faessler, T. Gutsche, S. Kovalenko, V. E. Lyubovitskij, I. Schmidt, and F. Simkovic, Phys. Rev. D **70**, 055008 (2004), hep-ph/0405164.
 [63] A. Faessler, T. Gutsche, S. Kovalenko, V. E. Lyubovitskij, I. Schmidt, and F. Simkovic, Phys. Lett. B **590**, 57 (2004), hep-ph/0403033.
 [64] V. M. Budnev, I. F. Ginzburg, G. V. Meledin, and V. G. Serbo, Phys. Rept. **15**, 181 (1975).
 [65] Y.-S. Tsai, Rev. Mod. Phys. **46**, 815 (1974), [Erratum: Rev.Mod.Phys. 49, 421–423 (1977)].

- [66] J. D. Bjorken, R. Essig, P. Schuster, and N. Toro, Phys. Rev. D **80**, 075018 (2009), 0906.0580.
- [67] Y.-S. Liu and G. A. Miller, Phys. Rev. D **96**, 016004 (2017), 1705.01633.
- [68] A. S. Zhevlakov, D. V. Kirpichnikov, and V. E. Lyubovitskij, Phys. Rev. D **106**, 035018 (2022), 2204.09978.
- [69] V. Shtabovenko, R. Mertig, and F. Orellana, Comput. Phys. Commun. **207**, 432 (2016), 1601.01167.
- [70] V. Shtabovenko, Comput. Phys. Commun. **218**, 48 (2017), 1611.06793.
- [71] V. Shtabovenko, R. Mertig, and F. Orellana, Comput. Phys. Commun. **256**, 107478 (2020), 2001.04407.
- [72] E. Byckling and K. Kajantie, *Particle Kinematics* (University of Jyväskylä, Jyväskylä, Finland, 1971).
- [73] Y. M. Andreev et al. (NA64), Phys. Rev. Lett. **131**, 161801 (2023), 2307.02404.
- [74] H. Sieber, D. V. Kirpichnikov, I. V. Voronchikhin, P. Crivelli, S. N. Gninenko, M. M. Kirsanov, N. V. Krasnikov, L. Molina-Bueno, and S. K. Sekatskii, Phys. Rev. D **108**, 056018 (2023), 2305.09015.
- [75] T. Åkesson et al. (LDMX Collaboration), JHEP **04**, 003 (2020), 1912.05535.